Wide- and Narrow-Band Bandpass Coplanar Filters in the W-Frequency Band

Eric Rius, Gaëtan Prigent, Henri Happy, Gilles Dambrine, Samuel Boret, and Alain Cappy

***Abstract*—This paper deals with the design of passive coplanar devices in the W-frequency band. As long as coplanar transmission lines are correctly dimensioned, analytical models based on quasi-TEM approximation can be used. Such models are associated with a correct definition of the reference planes at the junctions and employed for junction discontinuities, T- and cross-junctions. In order to validate these assertions, simulated and experimental data on classical quarter-wavelength shunt-stub filters are first presented. Then the design of traditional coupled-line filters is examined. The problems in terms of insertion loss associated with these kinds of narrow-band applications are discussed here. Minimization of insertion losses requires increasing the width of the strips. Consequently, the design becomes complex and modeling using transmission-line models less accurate. Nevertheless, as an optimization procedure is needed to tune the filter theoretically, such a very fast design method is necessary. Simulated and experimental results in the range 500 MHz to 110 GHz are compared throughout the paper.**

***Index Terms*—Bandpass filter, coplanar technology, monolithic microwave integrated circuit (MMIC), W-frequency band.**

I. Introduction

During the past decade, the W-band (75–110 GHz) frequency range was mainly allocated to military applications. Nowadays, civil applications such as collision avoidance radar and passive imaging systems are being developed using the specific properties of free space propagation in the W-band. In this frequency range, a high-level technological resolution process is needed at low wavelengths. This means that millimeter-wave monolithic integrated circuits (MWMICs) are generally preferred to hybrid technology. Moreover, coplanar waveguides are more currently used in the design of such circuits [1]–[6].

Many studies have, indeed, shown that coplanar waveguides can be considered as a good alternative to microstrip lines in the millimeter frequency range [7]–[14]. Because all conductors are located on the same plane, the ground connections through via-holes are eliminated and no reverse side processing is needed, which significantly reduces cost. Because of the large decoupling between the different elements of a coplanar system, global size reduction may be obtained as well. Another advantage of the coplanar technology is flexibility in the design of the passive circuits. Indeed, a large number of geometrical parameters can be chosen to design a transmission line with a given impedance. Electrical characteristics can then be improved by correctly defining the ratio between the strip width and the slot width.

However, designers are faced with two major drawbacks when they deal with coplanar technology. The first one is the lack of mature equivalent-circuit models like those available for microstrip lines. The second one concerns the suppression of the fundamental, but parasitic, slotline mode that may be excited by nonsymmetrical coplanar waveguide discontinuities such as, for example, bends or T-junctions. The suppression of such perturbing modes is achieved by inserting bridges over the center conductor, so that the potentials either side of the lateral ground planes are identical [15], [16]. Consequently, additional steps in the production process are needed for the fabrication of the bridges.

This paper is aimed at demonstrating that the methods used when designing coplanar passive devices for centimetric frequencies are also available for millimetric frequencies up to W-band. In fact, when cross-section dimensions are correctly chosen, coplanar transmission lines exhibit low dispersion up to W-band. Consequently, quasi-TEM analytical transmission-line models associated with specific design rules for the discontinuities are commonly used. Such methods are not only well suited for designing completely passive functions, but also very convenient for circuit optimization. However, in the case of narrow-band applications, insertion losses become the major problem. The designer must try to minimize these, and consequently the resulting geometry may not match up to the specific rules originally defined. The design is more complex and the modeling less accurate. In fact, the problems met in W-band are the same as in the centimetric wave range.

To develop these ideas, we first describe the technological process used and report on preliminary measurements made on both transmission lines and parallel stubs to verify the electrical behavior of T- and cross-junction discontinuities. Then, experimental and simulated data are compared over a broad frequency range; the center frequencies of the stubs are located in the W-band around 75 GHz.

In the second part, we describe the study of traditional quarter-wavelength shunt-stub filters [17] using the stubs described above. Experimental results obtained on three filters centered in W-band with 82%, 58%, and 36% 3-dB bandwidths are presented. They fit simulated data and validate the very simple design principle which appears to be sufficient, giving

Manuscript received December 6, 2001; revised September 20, 2002.

E. Rius and G. Prigent are with the Laboratoire d'Electronique et des Systèmes de Télécommunication (LEST), BP 809, 29285 Brest, France (e-mail: eric.rius@univ-brest.fr).

H. Happy, G. Dambrine, and A. Cappy are with the Institut d'Electronique de Microélectronique et de Nanotechnologie (IEMN), 59652, Villeneuve d'Asq, France.

S. Boret was with the Institut d'Electronique de Microélectronique et de Nanotechnologie (IEMN), 59652, Villeneuve d'Asq. He is now with STMicroelectronics, F-38926 Crolles, France.

Digital Object Identifier 10.1109/TMTT.2003.808586

the low sensitivity of the topology. These filters are dedicated to wide-band applications. For all the paper, the filter bandwidths are taken at 3 dB under insertion losses.

The case of narrow-band applications is examined in the last part in which we present results for traditional coupled-line filters [17]. Regarding the critical point of insertion losses whose level is closely related to the filter selectivity, the design for such applications is very sensitive. To achieve a sufficiently low insertion loss level, it is necessary to increase the strip width. However, this raises important problems concerning the modeling, the influence of the reverse side of the substrate, and the mechanical stability of the bridges. These points are discussed in detail here. We have clearly demonstrated the great flexibility of the coplanar technology up to W-band, but a limit is reached. Thus, new technological concepts are needed to continue the work.

II. Transmission Lines and Junction Discontinuities

The circuits presented in this paper are made on a 400-μm GaAs substrate using 700-Å Ni adhesion film base and 3-μm-thick electroplated gold. A second electroplated gold process is required to fabricate the air bridge [18]. The resolution of this technological process is about 1 μm for both strips and slots.

The cross-section design of coplanar waveguides constitutes an important part of efficient MMIC development. One can preserve low-dispersion quasi-TEM mode by carefully choosing the line geometry defined by d, w, s, w_g, and h_s where d is the ground-to-ground distance, w is the central strip width, s is the slot width, w_g is the ground width, and h_s is the substrate thickness. The parameters d and w_g are chosen to make a tradeoff between losses and low dispersion up to the W-frequency band. The following conditions:

$$d = (w + 2s) \leq \frac{\lambda_g}{10} \tag{1}$$

$$w_g > w + 2s \tag{2}$$

$$h_s \geq 2(w + 2s) \tag{3}$$

where λg is the dielectric wavelength are used [19]. For a 50-Ω CPW transmision line built on a 400-μm GaAs substrate and with a strip width of 26 μm, the dielectric wavelength is 1.6 mm at 75 GHz.

In order to minimize the parasitic influence of the bridge on the electrical characteristic of the lines and provide mechanical stability, the dimensions of the air bridge used are: 3-μm height, 10-μm width, 80-μm (70 + 10 minimum) length, and 3-μm metal thickness. Moreover, to give it a good mechanical stability, a maximum length must be defined for a given width: for example, 10-μm and 20-μm widths allow maximum lengths of 100 and 180 μm, respectively. Although the bridge introduces an excess capacitance, this does not constitute a problem for the bridge widths here as long as the strip widths of the coplanar line are all kept small. Under a configuration with these dimensions, no compensation techniques, such as using sections of high-impedance line, are required [20], [21]. An example of this realization is shown in Fig. 1.

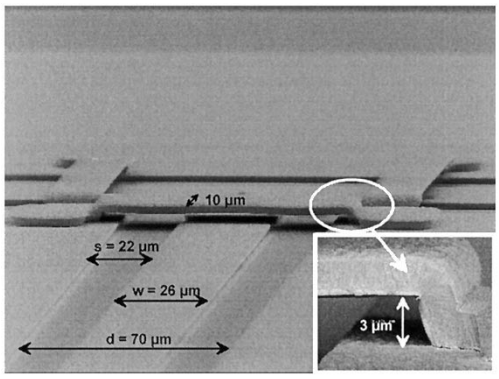

Fig. 1. Bridges on a 50-Ω CPW, T-junction discontinuity.

According to (1)–(3), several lines are tested. The ground plane width is 200 μm. Characteristic impedances of 30, 50, and 70 Ω are achieved by using strip widths of 54, 26, and 10 μm, respectively, along with a ground-to-ground spacing of 70 μm. These dimensions are obtained using traditional analytical TEM models available on commercial CAD software such as Agilent-ADS [22]. These models are based on conformal mapping [23] in which corrections are added to take into account the influence of the metallization thickness. As these models are quasi-static, they do not take into account possible frequency dependence. With these dimensions, our transmission lines are within the validity domain of the models. The effective line length is 480 μm. On-wafer measurements are made from 500 MHz to 110 GHz on HP 8510B using TRL calibration. Standards for TRL calibration are fabricated on the same wafer.

Fig. 2(a) and (b) presents experimental and simulated results on 50- and 70-Ω CPW transmission lines, respectively. Fig. 2(a) exhibits a good matching level and correct insertion losses. The return losses over the whole frequency measurements obtained are at least 25 dB, and the line attenuation is about 0.4 dB/mm at 94 GHz. Fig. 2(b) shows complete agreement between the measurement and the TEM transmission line simulation. Other experiments were conducted to verify the effect of one and then several bridges on the electrical characteristics of such transmission lines.

Systematic investigations are carried out on stubs: 30-, 50-, and 70-Ω simple, double, shorted, and open stubs are then made. Their lengths are such that they exhibit a resonant frequency of about 75 GHz in the W-band. This allow us to study the electrical behavior of T- and cross-junction discontinuities. Fig. 3(a)–(d) presents the experimental results obtained by using 50-Ω shorted and opened double and simple stubs, respectively. One should note a significant difference between the circuits including T-junction and those with cross-junction. The measured resonant frequencies of double and simple stubs are 77.15 and 72.77 GHz, respectively. Since the resonant frequency is the same for a given junction topology, regardless of stub ending, the open and shorted ends should be equivalent in term of excess length.

Thus, according to this great difference T- and cross-junction discontinuities exhibit totally different electrical behaviors. Our purpose here is not to perform a rigorous physical analysis of this problem but to propose a simple way of modeling these

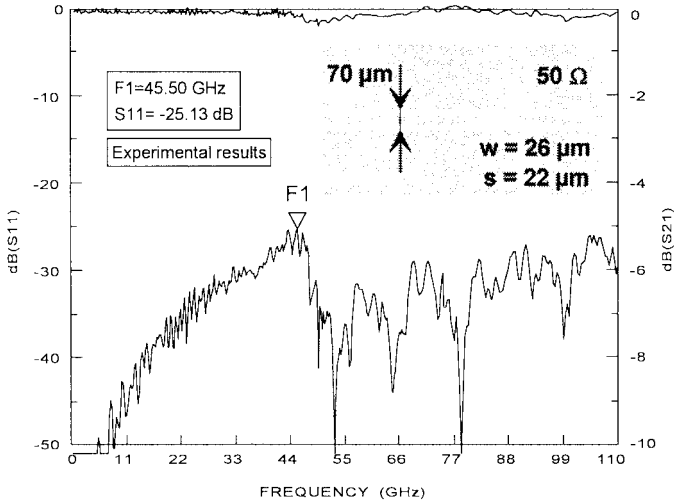

(a)

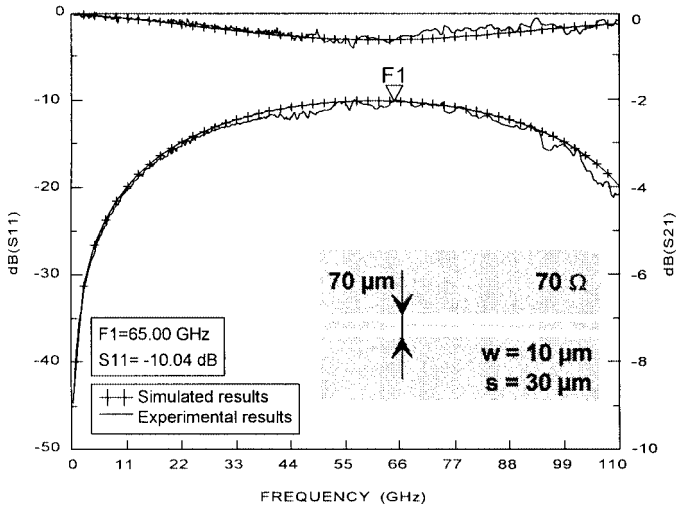

(b)

Fig. 2. (a) Experimental frequency responses on a 50-Ω CPW transmission line. (b) Experimental and simulated frequency responses on a 70-Ω CPW transmission line.

phenomena. In fact, stubs are modeled only with TEM transmission lines. In simulation, the effect of the discontinuities (junction and ending) is taken into account by defining the reference planes at the center of junction discontinuity in Fig. 3(a)–(d) for cross-junctions and T-junctions, the lengths of the stubs being choosen different for the two cases. As illustrated in the four examples of Fig. 3, a correct fit with experimental results is obtained. This agreement is also valid for the phase parameters. We also tested this method for other characteristic impedances, 30 and 70 Ω, while keeping the ground-to-ground spacing constant at 70 μm. The agreement is the same as in the 50-Ω case. Concerning the validity domain of this method, it is obvious that the cross-section dimensions are critical parameters. In fact, this method is not valid for large ground-to-ground spacing.

III. Wide-Band Bandpass Filter

This section is dedicated to the design of quarter- wavelength shunt-stub filters using the stubs studied above. Such topology includes shorted stubs as resonators separated by quarter-wavelength transmission lines as inverters. The synthesis due to Matthaei [17] indicates that the bandwidth is in close relation with the impedance level of the resonators. In the present case, if the impedance range extends from 30 to 70 Ω, the available 3-dB bandwidth will be approximately bounded by 100% and 36%. These values are given approximately for return losses chosen around 20 dB. For bandwidths below 36%, very low impedance levels are needed. Thus, shape factors become too large for correct performance from the device with regard to both the parasitic influences of the discontinuities and modeling difficulties. So, other topologies such as coupled-line filters are preferred. They will be used in the next part of this study.

The first results presented here deal with an 82%, 3-dB-bandwidth, third-order filter centered on 78 GHz. According to the synthesis procedure, it is composed of two 53-Ω inverters and three 50-Ω resonators. The sensitivity of this device being very low, an impedance of 50 Ω can be chosen for all the constitutive elements of the filter without causing any damage on the frequency response. Moreover, as wide-band filters do not exhibit high insertion losses, the cross section of the line and, especially, the strip widths are free from constraints. So, along the filter and access lines the strip and slots widths chosen for standard geometry are 26 and 22 μm, respectively. As defined by the layout, the resonators and inverters are 393 and 380 μm long. As mentioned above (Section II), quasi-TEM lines associated with correct design rules for the discontinuities are sufficient to simulate the filter. The simulation model and the associated layout are presented in Fig. 4. Experimental and simulated results are in good agreement (Fig. 5). The phase response is in similar agreement. Moreover, this agreement is valid on a large frequency band from 500 MHz to 110 GHz. Insertion losses are 0.53 dB at 78 GHz, and return losses better than 20 dB are obtained all over the bandwidth.

Two others examples of filters centered on an equivalent frequency are presented in Figs. 6 and 7. They are 58% and 36% 3-dB-bandwidth. The first example with 58% 3-dB-bandwidth results in a 25-Ω impedance for the resonators when inverters are kept to 51 Ω. Twenty-five Ω is chosen so as to introduce double 50-Ω stubs for the resonator (Fig. 6). According to the low level of insertion losses, the standard geometry was chosen as follows: 26 μm for the strip widths and 22 μm for the slot widths. The 36% bandwidth was reached by selecting impedances of 56 and 15 Ω for inverters and resonators, respectively. As before, 15 Ω was obtained with two double 30-Ω stubs. It corresponds to the lowest bandwidth that can be reached with an impedance range bounded by 30 and 70 Ω. For the inverters, strips and slots were 20 and 25 μm, respectively, and 54 and 8 μm for the resonators. The layout and frequency response are displayed in Fig. 7. As for the first prototype, experimental and simulated results agree over a broad-band frequency. As shown in Figs. 5–7, insertion losses increase with filter selectivity: 0.68, 0.96, and 1.81 dB are obtained for 82%, 58%, and 36% bandwidth filters, respectively. These values are in complete agreement with the following expression [17], [24]:

$$I.L = \frac{4.343 \cdot n}{Qu \cdot w}. \tag{4}$$

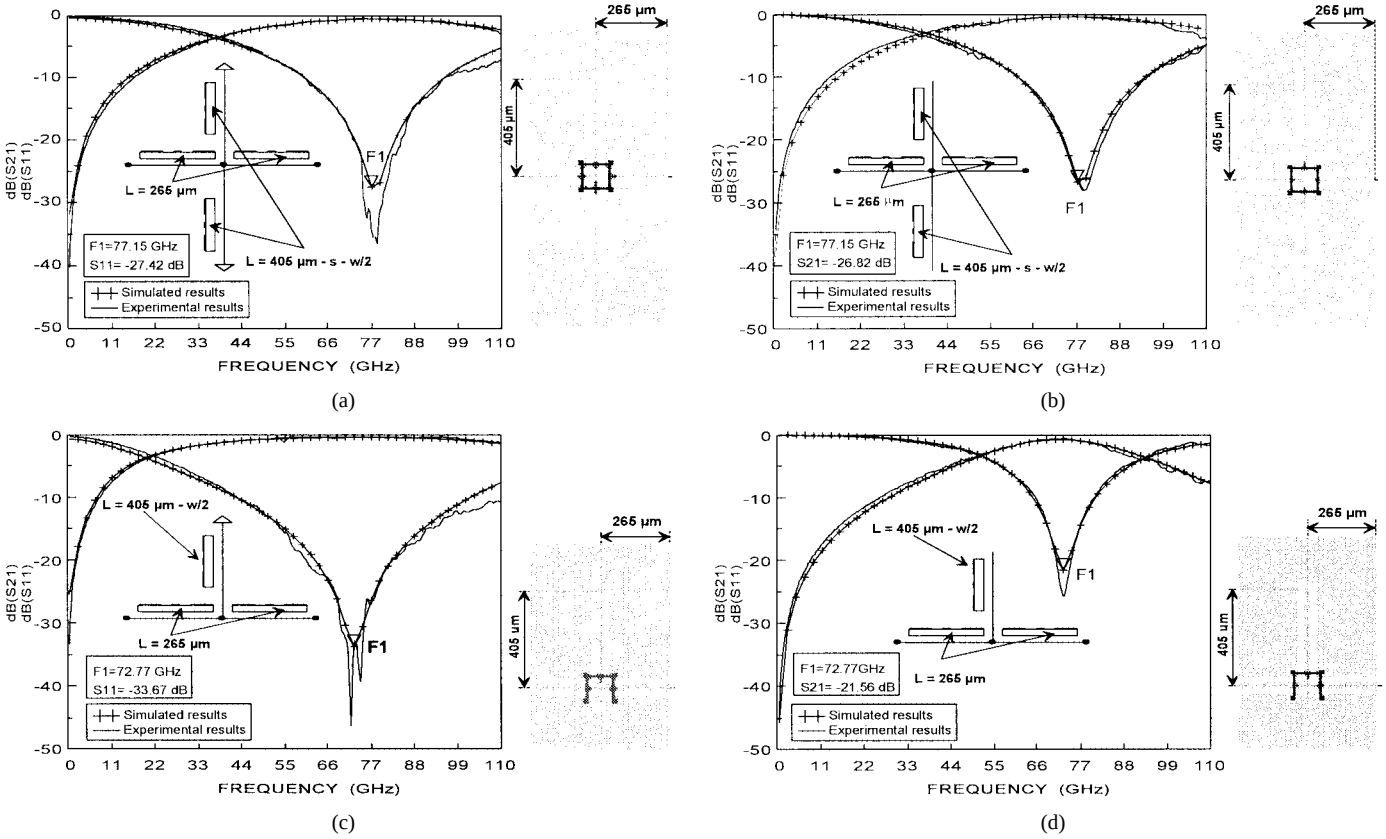

Fig. 3. Experimental and simulated results on different stub configurations in W-frequency band. (a) Double shorted stubs. (b) Double opened stubs. (c) Simple shorted stub. (d) Simple opened stub.

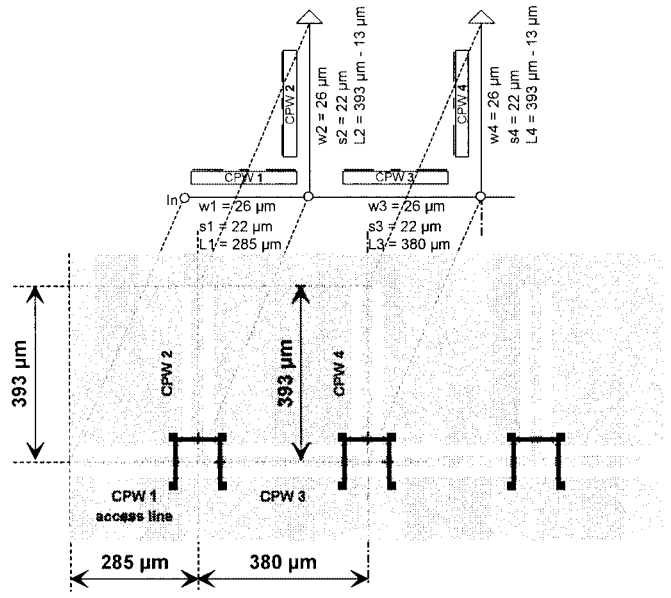

Fig. 4. Layout and electrical model of the 78-GHz central-frequency, 82% 3-dB-bandwidth, third-order quarter-wavelength shunt-stubs filter with associated access lines.

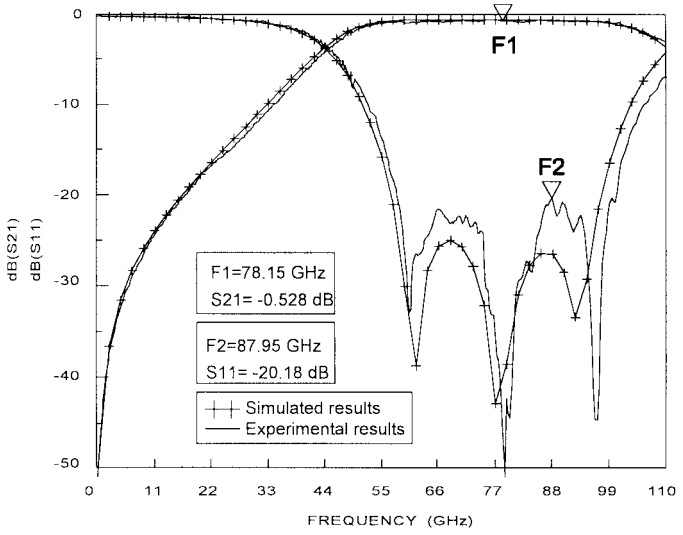

Fig. 5. Simulated and experimental magnitude responses of the 78-GHz central-frequency, 82% 3-dB-bandwidth filter.

In this formula, $I.L$ is the insertion loss in decibels, n is the filter order, w is its relative bandwidth, and Qu is the unloaded quality factor, which is close to 25 for the standard 50-Ω transmission line used here. On the other hand, as equal resonator lengths of 393 μm were chosen for the three examples, the filter with T-junctions exhibits a 78-GHz central frequency whereas the filters with cross-junctions exhibit 82.7-GHz center frequencies. This difference is in agreement with the difference already observed in Section II concerning the discontinuities.

IV. Narrow-Band Bandpass Filter

Two major problems are related to narrow-band bandpass coupled-lines filters. First, insertion losses become important when the selectivity of the filter is increased. The second

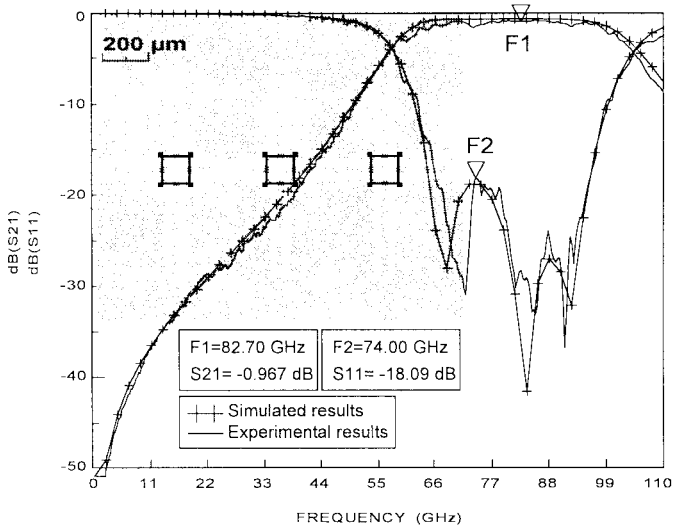

Fig. 6. Layout, simulated, and experimental associated magnitude responses of the 82.7-GHz central-frequency, 58% 3-dB-bandwidth filter.

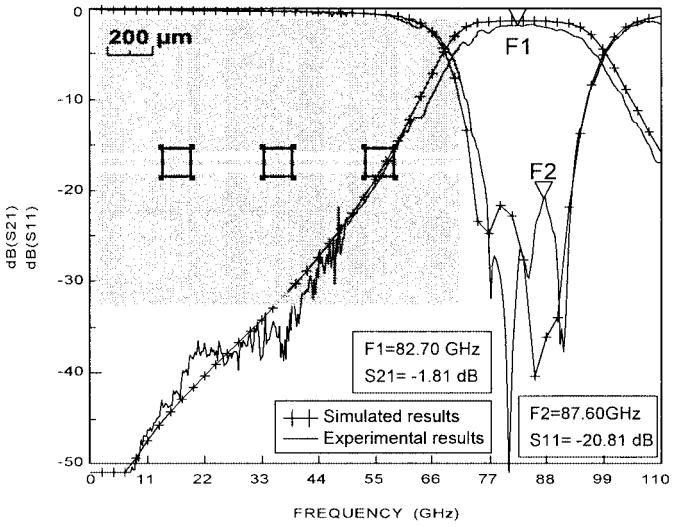

Fig. 7. Layout, simulated, and experimental associated magnitude responses of the 82.7-GHz central-frequency, 36% 3-dB-bandwidth filter.

problem deals with accuracy which is directly in relation to the level of selectivity.

In order to illustrate this, we present the results obtained with two classical coupled-lines third-order bandpass filters. The first one is at a center frequency of 65 GHz, 22% 3-dB bandwidth whereas the second one is at 94 GHz, 5% 3-dB bandwidth. Figs. 8 and 10 show the layouts of these filters. For such topologies, according to the well-known synthesis of Matthaei, the bandwidth and the coupling coefficient level of the coupled-lines sections are in close relation [17]. Indeed, narrow selective bandwidths are obtained with low coupling levels on the central sections of the filter. A convenient solution consists of using a separating ground plane between the coupled strips. This leads to low coupling levels on a reduced bulk and this separate ground plane acts as a good parasitic mode filter (Fig. 10).

According to the finite conductivity of the metal (2.5×10^7 S.m^{-1} for gold metallization) and to the $\tan\delta$ (0.0003) of the GaAs substrate, very high insertion losses

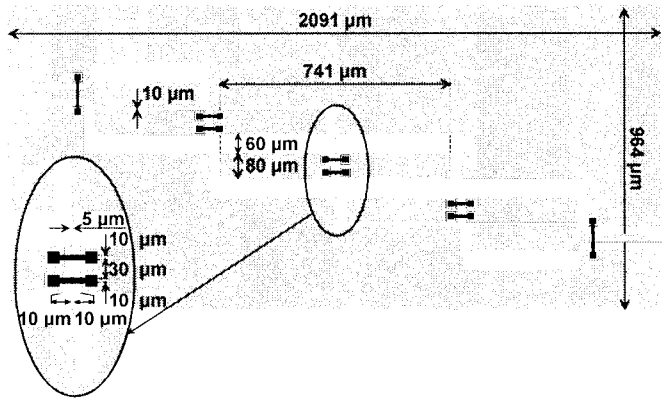

Fig. 8. Layout of a 65-GHz central-frequency, 22% 3-dB-bandwidth, coupled-line filter.

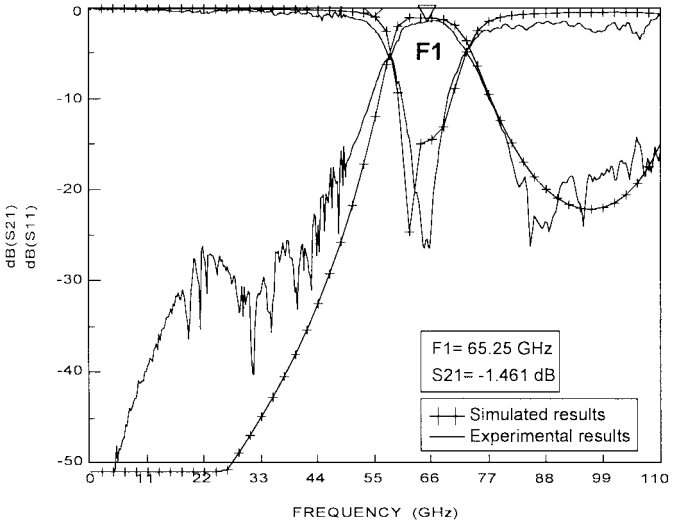

Fig. 9. Simulated and experimental magnitude responses of the 65-GHz central-frequency, 22% 3-dB-bandwidth, coupled-line filter.

are expected when designing such narrow-band filters. These insertion losses can be predicted roughly from (4). For instance, for a third-order, 22% 3-dB-bandwidth coupled-line filter designed with 26-μm strip widths, insertion losses between 1.95 and 2.95 dB are obtained. However, if the bandwidth is decreased to 5%, insertion losses reach a critical level between 8.7 and 13 dB. These values were calculated with the unloaded quality factor of 20 and 30. One way of improving this critical point is to increase the strip widths, but this gives rise to several problems.

The first problem concerns the bridge topology: a large ground-to-ground spacing is, indeed, forbidden because of mechanical stability constraints. A good way to solve this problem is to fabricate an inter-strip bridge as shown in Figs. 8 and 10. By doing so, the ground connections used for filtering the coupled-slotline modes are made directly with a tiny strip on the first metallization layer. In this case, the bridge length is about 10% of the total length of a resonator. According to the high selectivity of the filter, this length must be taken into account, which can be done by cascading several different section line topologies consisting of coupled strips on substrate and a coupled air-filled microstrip line.

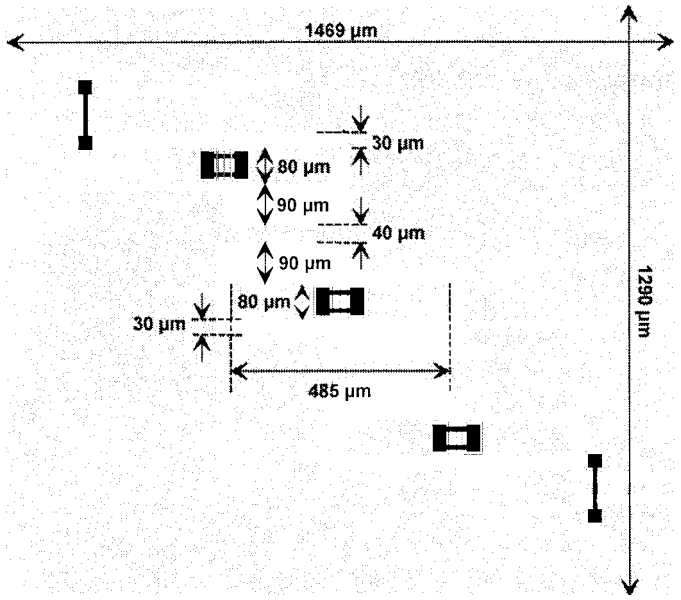

Fig. 10. Layout of a 94-GHz central-frequency, 5% 3-dB-bandwidth, coupled-line filter.

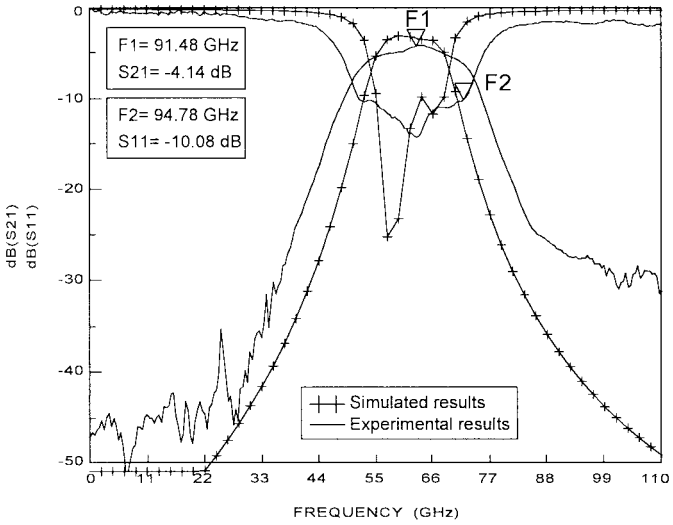

Fig. 11. Experimental and postsimulation results of the 94-GHz central-frequency, 5% 3-dB-bandwidth, coupled-line filter.

The second one concerns modeling. Obviously, as the strips are wider, the conditions of low dispersion given in Section II are not necessarily still valid. Moreover, the validity conditions of the analytical quasi-TEM models used are not always met. Finally, the dimensions of the discontinuities increase with the strip widths and, consequently, strong parasitic effects appear. Modeling them accurately with a simple approach similar to the one described in Section II is quite difficult and it allows only an approximation. Nevertheless, as an optimization procedure is needed to adjust all the characteristics of the filter response correctly, it requires the use of a very fast modeling technique. After this optimization phase, there is nothing to prevent the designer from completing the modeling with an electromagnetic method. Useful libraries dedicated to multilayer and multiple-coupled lines are now available on commercial CAD software and allow one to describe a wide range of coplanar or other planar geometries with a static approach [25].

As shown in Fig. 9 for the 22% 3-dB-bandwidth prototype, a good agreement is observed between simulated and experimental results. The phase response is in similar agreement. This agreement is valid over a wide frequency band from 500 MHz to 110 GHz and, as expected, correct insertion loss levels of about 1.4 dB are observed in the bandwidth.

Since the bandwidth is very selective, the measurements were only made on a frequency range from 66 to 110 GHz for the second prototype. The experimental results are presented in Fig. 11 and give a 4-dB insertion loss and 10-dB return loss for a center frequency of 91.5 GHz. Compared to the expected results, one should also note a significant bandwidth broadening. In this case, this problem is only due to the reverse side of the substrate. Indeed, as the ground-to-ground spacing is very large, the electromagnetic fields are strongly modified by the electrical condition on the reverse side of the dielectric substrate: open or grounded. Impedance and coupling levels are subject to changes that significantly modify the frequency response. Postsimulation was carried out to check the bandwidth broadening by taking into account correct conditions on the substrate backside. This postsimulation is presented in Fig. 11. As this problem masks the errors due to the modeling method, it is difficult to form any conclusions regarding its accuracy in this frequency range. One should only note the validity of this very simple and fast method. Although the insertion loss appears to be correct, new experiments on filters with a correct bandwidth and return loss are necessary to assess the insertion loss accurately.

Nevertheless, when designing future very high-selectivity filters for which the confinement of the electromagnetic field is a problem, the designer must keep in mind the packaging aspect. As grounded CPW lines are not a very convenient solution, three-dimensional technological solutions using, for instance, thin- or thick-film microstrip transmission lines appear to be equally well suited [26]–[30].

V. Conclusion

Compared to traditional microstrip technology, the flexibility of coplanar technology is an important advantage for the design of filter in high frequency range. Choosing suitable cross-section dimensions avoids dispersion and allows the use of analytical quasi-TEM models. The association of such models with specific design rules for describing electrical discontinuity constitutes a very convenient method for passive device design. We have seen its efficiency for the design of wide-band filters on a broad-band frequency range: within 500 MHz and 110 GHz and a good agreement between experimental results and theoretical predictions was obtained. However, the design of very narrow-band applications is much more difficult because of the levels of sensitivity and insertion loss. In order to optimize the latter, the strips have to be widened, as well as changes made to the bridge topology. Moreover, electrical conditions on the reverse side of the substrate must be taken into account and modeling with transmission-line models becomes less accurate. Nevertheless, as an optimization procedure is needed to tune the filter theoretically, a very fast modeling technique must be

used. In fact, since the structures are complex and the shape ratios high, electromagnetic global analysis is not well suited. As shown on this paper, coplanar coupled-line filters do not constitute the definitive solution for narrow-band application. In order to design such critical devices, it is necessary to develop new technological concepts, such as multilayer or three-dimensional technology. In the image of coplanar technology, the intrinsic qualities of these new technological solutions must be low dispersion over a broad-band frequency range and very high level of flexibility.

ACKNOWLEDGMENT

The authors thank R. Jezequel from LEST and S. Lepilliet and B. Grimbert from IEMN for measurements and circuit realization.

REFERENCES

[1] V. Hoel, S. Boret, B. Grimbert, G. Aperce, S. Bollaert, H. Happy, X. Wallart, and A. Cappy, "94-GHz low noise amplifier on InP in coplanar technology," in *Proc. Microwave Engineering Europe*, Nov. 1999, pp. 51–54.

[2] T. Sporkmann and N. Naghed, "Coplanar MMICs—The future for mass production," in *Proc. GAAS 98*, Amsterdam, The Netherlands, pp. 236–251.

[3] B. Argarwal, A. E. Schmitz, J. J. Brown, M. Matloubian, M. G. Case, M. Le, M. Lui, and M. J. W. Rodwell, "112-GHz, 157-GHz, and 180-GHz InP HEMT traveling-wave amplifiers," *IEEE Trans. Microwave Theory Tech.*, vol. 46, pp. 2553–2559, Dec. 1998.

[4] W. H. Haydl, M. Neumann, L. Verveyen, A. Bangert, S. Kudszus, M. Schlechtweg, A. Hülsmann, A. Tessmann, W. Reinert, and T. Krems, "Single-chip coplanar 94-GHz FMCW radar sensors," *IEEE Microwave Guided Wave Lett.*, vol. 9, pp. 73–75, Feb. 1999.

[5] T. Hirose, K. Makiyama, K. Ono, T. M. Shimura, S. Aoki, Y. Ohashi, S. Tokokawa, and Y. Watanabe, "A flip-chip MMIC design with coplanar waveguide transmission line in the W-band," *IEEE Trans. Microwave Theory Tech.*, vol. 46, pp. 2276–2282, Dec. 1998.

[6] J. Papapolymerou, F. Brauchler, J. East, and L. P. B. Katehi, "W-band finite ground coplanar monolithic multipliers," *IEEE Trans. Microwave Theory Tech.*, vol. 47, pp. 614–619, May 1999.

[7] M. Houdard, "Coplanar lines: Application to broadband microwave integrated circuits," in *Proc. Eur. Microwave Conf.*, 1976, pp. 49–53.

[8] T. Hirota and H. Ogawa, "Uniplanar MMIC hybrids—A proposed new MIC structures," *IEEE Trans. Microwave Theory Tech.*, vol. 35, pp. 576–581, June 1987.

[9] H. Ogawa and A. Minagawa, "Uniplanar MIC balanced multiplier—A proposed new structure for MIC's," *IEEE Trans. Microwave Theory Tech.*, vol. MTT-35, pp. 1363–1368, Dec. 1987.

[10] A. K. Rayit and N. J. McEwan, "Coplanar waveguide filters," in *Proc. Microwave Theory Tech. Symp.*, Atlanta, GA, 1993, pp. 1317–1320.

[11] F. Brauchler, S. Robertson, J. East, and L. P. B. Katehi, "W band FGC line circuit elements," in *Proc. Microwave Theory Tech. Symp.*, San Francisco, CA, 1996, pp. 1845–1848.

[12] R. Kulke and I. Wolff, "Design of passive coplanar filters in V band," in *Proc. IEEE MTT-S Int. Microwave Symp. Dig.*, San Francisco, CA, 1996, pp. 1647–1650.

[13] K. J. Herrick, T. Schwarz, and L. P. B. Katehi, "Si-Micromachined coplanar waveguide for use in high-frequency circuit," *IEEE Trans. Microwave Theory Tech.*, vol. 46, pp. 762–768, June 1998.

[14] K. Hettak, N. Dib, A. Omar, G. Y. Delisle, M. Stubbs, and S. Toutain, "A useful new class of miniature CPW shunt stubs and its impact on millimeter-wave integrated circuits," *IEEE Trans. Microwave Theory Tech.*, vol. 47, pp. 2340–2349, Dec. 1999.

[15] N. H. L. Koster, S. Koslowski, R. Bertenburg, S. Heinen, and I. Wolff, "Investigation on airbridges used for MMIC's in CPW technique," in *Proc. Eur. Microwave Conf.*, 1989, pp. 666–671.

[16] K. Beilenhoff, W. Heinrich, and H. L. Hartnagel, "The scattering behavior of air bridges in coplanar MMICs," in *Proc. Eur. Microwave Conf.*, vol. II, 1991, pp. 1131–1135.

[17] G. Matthaei, L. Young, and E. M. T. Jones, *Microwave Filters, Impedance-Matching Networks, and Coupling Structures*. Dedham: Artech House, 1980.

[18] S. Boret, L. Kadri, F. Huret, H. Happy, G. Dambrine, A. Cappy, P. Kennis, and E. Rius, "Modeling of passive coplanar elements for W-band ICS, experimental verification up to 110 GHz and parasitic mode coupling," in *Proc. Eur. Microwave Conf.*, 1998, pp. 190–195.

[19] W. Heinrich, "Quasi-TEM description of MMIC coplanar lines including conductor-loss effects," *IEEE Trans. Microwave Theory Tech.*, vol. 41, pp. 45–52, Jan. 1993.

[20] E. Rius, J. P. Coupez, S. Toutain, C. Person, and P. Legaud, "Theoretical and experimental study of various dielectric bridges for millimeter-wave coplanar application," *IEEE Trans. Microwave Theory Tech.*, vol. 48, pp. 152–156, Jan. 2000.

[21] T. M. Weller, R. M. Henderson, K. J. Herrick, S. V. Robertson, R. T. Kihm, and L. P. B. Katehi, "Three-dimensional High-frequency distribution network—Part I: Optimization of CPW discontinuities," *IEEE Trans. Microwave Theory Tech.*, vol. 47, pp. 614–619, May 1999.

[22] ADS 1.5, "Advanced Design System," Agilent Technol., Palo Alto, CA.

[23] C. P. Wen, "Coplanar waveguide: A surface strip transmission line suitable for non reciprocal gyromagnetique devices applications," *IEEE Trans. Microwave Theory Tech.*, vol. MTT-17, pp. 1087–1090, Dec. 1969.

[24] S. B. Cohn, "Dissipation loss in multiple-coupled-resonator filters," in *Proc. IRE*, vol. 47, Aug. 1959, pp. 1342–1348.

[25] Multilayer Interconnect Library, Agilent Technol., Palo Alto, CA.

[26] E. Rius, C. Person, T. Le Nadan, C. Quendo, and J. P. Coupez, "3. D integrated narrowband filters for millimeter-wave wireless applications," in *Proc. Microwave Theory Tech. Symp.*, Boston, MA, June 2000, pp. 323–326.

[27] G. Six, M. Vanmackelberg, H. Happy, G. Dambrine, S. Boret, and D. Gloria, "Transmission lines on low resistivity silicon substrate for MMIC's application," in *Proc. Eur. Microwave Conf.*, 2001, pp. 193–196.

[28] M. S. Aftanasar, P. R. Young, I. D. Robertson, J. Minalgiene, and S. Lucyszyn, "Photoimageable thick-film millimeter-wave metal-pipe rectangular waveguides," *Electron. Lett.*, vol. 37, no. 18, pp. 1122–1123, Aug. 30, 2001.

[29] C. Warns, W. Menzel, and H. Schumacher, "Transmission lines and passive elements for multilayer coplanar circuits on silicon," *IEEE Trans. Microwave Theory Tech.*, vol. 46, pp. 616–622, Jan. 2000.

[30] F. Schnieder and W. Heinrich, "Model of thin-film microstrip line for circuit design," *IEEE Trans. Microwave Theory Tech.*, vol. 49, pp. 104–110, Jan. 2001.

Eric Rius was born in Auray, France, on March 6, 1966. He received the Ph.D. degree in electronics from the University of Brest, Brest, France, in 1994.

Since 1995, he has been an Assistant Professor with the Electronic Department, Université de Bretagne Occidentale, Brest, France, and he currently conducts research with the Laboratory of Electronics and Communications systems (LEST). His research activities principally concern the design of filters and associated RF modules for microwave and millimeter-wave applications.

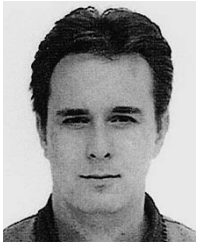

Gaëtan Prigent was born in Lannion, France, on December 2, 1973. He is currently working toward the Ph.D. degree at the Laboratory of Electronics and Communications Systems, Université de Bretagne Occidentale, Brest, France.

His research activities principally concern the modelization and design of planar filters for microwave and millimeter-wave applications.

Henri Happy was born in Yaoundé, Cameroun, on August 7, 1964. He received the Ph.D. degree from the Institut d'Electronique et de Microélectronique du Nord (IEMN), University of Lille, Lille, France, in 1992.

He is currently a Professor of Electronics at the University of Lille. His first research interests concerned HEMT modeling using a quasi-two-dimensional approach. He is one of the principal designers of the software HELENA(Hemt Electrical properties and Noise Analysis) published by Artech House. He is currently involved with the design and realization of monolithic microwave integrated ciruicts for optical communications systems using either planar or three-dimensional topologies.

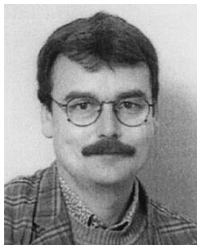

Gille Dambrine was born in Avion, France, on May 15, 1959. He received the Ph.D.degree and Habilitation à Diriger des Recherches (HDR) en Sciences degree from the Centre Hyperfréquences et Semiconducteurs, University of Lille, Lille, France, in 1989 and 1996, respectively.

He is currently a Professor of Electronics with the University of Lille. His main research interests concern the modeling, and characterization of ultimate low-noise devices for application in millimeter- and submillimeter-wave ranges. Over these last few years, his research interests are oriented to the characterization, including high-frequency noise, of advanced silicon devices.

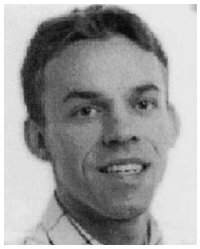

Samuel Boret was born in Malo-les-Bains, France, on December 23, 1972. He received the Ph.D. degree from the Centre Hyperfréquences et Semiconducteurs, University of Lille, Lille, France, in 1999.

As part of his graduate studies, he was involved with monolithic integrated circuits in coplanar technology for applications of reception up to 110 GHz. He is currently with Central Research and Development, RF Electrical Characterization Group, STMicroelectronics, Crolles, France. His main interests include design, characterization, and modeling of RF devices in advanced silicon technologies.

Alain Cappy was born in Chalons sur Marne, France, on January 25, 1954.

In 1977, he joined the Centre Hyperfréquences et Semiconducteurs, University of Lille, Lille, France. He is currently Professor of Electronics an Electrical Engineering with the University of Lille. His main research interests are concerned with the modeling, fabrication, and characterization of ultrahigh-speed device and circuits for applications in the centimeter and millimeter-wave ranges. He currently heads the Institute of Electronics, Microelectronics and Nanotechnology (IEMN), a research institute that gathers approximately 200 scientists and 100 Ph.D. students involved with microtechnology and nanotechnology, microelectronics and microsystems, telecommunication systems, and sensors. He has coauthored over 100 scientific papers and communications and has given 15 invited papers in international conferences and workshops.